NUMERICAL MODELING FOR CᴇꜱʀTA MEASUREMENTS OF ELECTRON CLOUD BUILDUP IN A QUADRUPOLE MAGNET

J.A. Crittenden, M.G. Billing, W.H. Hartung, C.S. Shill, J.P. Sikora and K.G. Sonnad
CLASSE*, Cornell University, Ithaca, NY 14853, USA

Abstract

We describe a numerical model for measurements of the formation of long-lived electron clouds in a quadrupole magnet in the CESR storage ring. The shielded stripline detector measures the electron flux incident on the vacuum chamber wall directly in front of one of the poles of the magnet. The model includes photoelectron production by synchrotron radiation, electrostatic forces from the bunched positron beam and the cloud, macroparticle tracking in the field of the quadrupole, secondary electron emission from the 9.5-cm-diameter cylindrical stainless steel beam-pipe and an analytic calculation of the transmission function of the holes in the vacuum chamber which allow cloud electrons to reach the stripline collector. These modeling studies provide a quantitative understanding of the trapping mechanism which results in cloud electrons surviving the 2.3 μs time interval prior to the return of a train of positron bunches. These studies have been performed in the context of the CESR Test Accelerator program, which aims to quantify and mitigate performance limitations on future low-emittance storage and damping rings.

INTRODUCTION

The Cornell Electron Storage Ring Test Accelerator (CᴇꜱʀTA) program [1] has been providing detailed measurements of electron cloud (EC) buildup in electron and positron beams with energies ranging between 1.9 and 5.3 GeV since 2008. In 2013, a shielded stripline detector was installed in a quadrupole magnet with a field gradient of 7.4 T/m, providing measurements of the time dependence of the buildup of the cloud. Electron cloud development results from photoelectron production by synchrotron radiation, from the EC dynamics in the electric fields of the beam and cloud and any ambient magnetic fields, and from the secondary yield (SEY) properties of the vacuum chamber. Along with these physical processes, the EC buildup simulation code ECLOUD [2] has been extended to model the response of the stripline detector. Here we describe its use to study the relationship between the cloud buildup and the detector signal in a quadrupole magnet for 20-bunch trains of 5.3 GeV positrons.

SHIELDED STRIPLINE DETECTOR

Figure 1a shows the circular stainless steel vacuum chamber of inner diameter 95.5 mm in the 60-cm-long quadrupole

magnet. The detectors are placed directly in front of magnet poles, as shown in Fig. 1b. Electrons are collected on the 7-mm-wide trace shown in Fig. 1c. This collector forms a transmission line with the grounded copper on the other side of the 0.12-mm-thick Kapton sheet. The tapered pattern is designed to limit reflections sufficiently to give a time resolution of about 10 ns. A pattern of 5 x 60 parallel holes 0.8 mm in diameter (see Fig. 1d) in the beam-pipe allows transmission of cloud electrons to the detector shown on the upper right in Fig. 1b. Cloud electrons which traverse the shielding holes are collected on the stripline, which is biased at 50 V relative to the vacuum chamber in order to prevent secondary
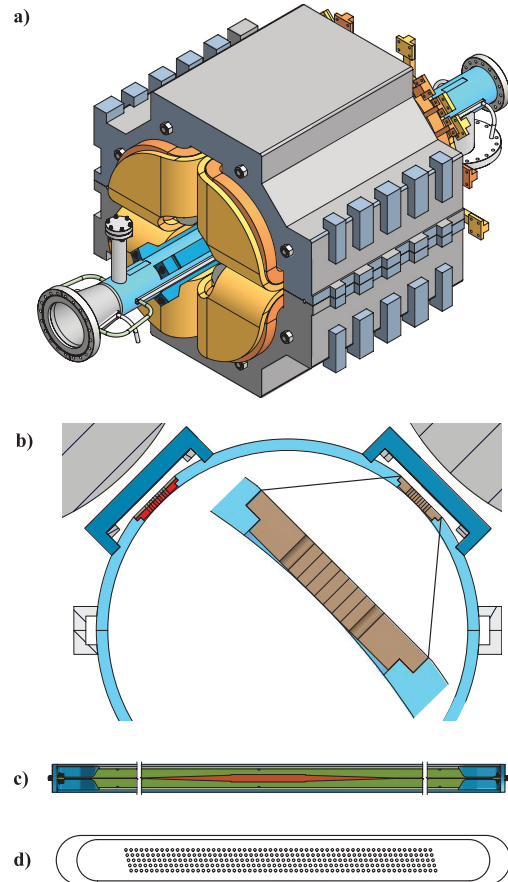

Figure 1: a) Vacuum chamber equipped with electron detectors in the quadrupole magnet. b) Arrangement of two detectors in front of the magnet poles as seen from the positron arrival direction. c) Geometry of the copper electrode biased at 50 V to collect electrons entering through the holes in the beam-pipe shown in d). The rectangular region of the collector and the pattern of holes are each about 10 cm long.

electrons from escaping. Two Mini-Circuits ZFL-500 broadband amplifiers with 50 Ω input impedance provide a voltage gain of 100 and drive the coaxial cable which transmits the signals to a digitizing oscilloscope. Oscilloscope traces are digitized to 8-bit accuracy in 1000 time bins 1.0 ns wide, averaging over 8000 triggers. The oscilloscope signals exhibit high-frequency beam-induced ringing following the passage of each bunch due to a high-pass characteristic of the stripline assembly. A 13 MHz low-pass digital filtering algorithm has been applied to the data, suppressing this noise by an order of magnitude.

ECLOUD MODELING CODE

The ECLOUD EC buildup simulation code has been employed to describe measurements with shielded button detectors in the arcs of the CESR ring [3–6], and time-resolved retarding field analyzer measurements with smooth and grooved aluminum vacuum chambers [7]. In order to tune the simulation to the measurements in the field of the quadrupole magnet, it was necessary to calculate the hole transmission factor averaged over the region of the shielding holes for a field of arbitrary magnitude aligned with the axis of the holes. For trajectories parallel to the field, the factor is simply the ratio of the fractional area of the holes, which is $S_\perp = 22\%$. To calculate the average fraction of electrons passing through holes as a function of incident polar angle θ_i ($\theta_i = 0$ for perpendicular incidence) and kinetic energy E_k, we convert θ_i, E_k to cyclotron radius R_c and the fractional number of cyclotron revolutions performed during wall traversal N_{rev}:

$$R_c = \frac{\sqrt{2mE_k}\sin\theta_i}{eB_\parallel}; \qquad N_{rev} = \frac{1}{2\pi}\frac{e}{\sqrt{2mE_k}}\frac{B_\parallel L_H}{\cos\theta_i}, \quad (1)$$

where m is the mass of the electron, e its charge, $B_\parallel$ the magnetic field strength and L_H is the hole depth, i.e. the vacuum chamber wall thickness. Comparing the cyclotron radius to the hole radius R_H, one can calculate the average hole transmission as $S_H = S_\perp S_{dyn}$ for two simple cases:

$$N_{rev} > \frac{1}{2}; \quad R_c > R_H : S_{dyn} = 0 \qquad (2)$$

$$N_{rev} > 1; \quad R_c < R_H : S_{dyn} = \left(1 - \frac{R_c}{R_H}\right)^2 \qquad (3)$$

For the case of large cyclotron radius and less than half a cyclotron revolution during wall passage, we can define the angle ϕ such that $\cos\phi/2 = \frac{R_c}{R_H}\sin\psi_{rev}/2$, where $\psi_{rev} = 2\pi N_{rev}$, which can be used to express the average fraction of hole area occupied by the cyclotron motion. We derive

$$N_{rev} < \frac{1}{2}; \quad R_c > R_H : S_{dyn} = \frac{1}{\pi}(\phi - \sin\phi) \qquad (4)$$

Finally, if less than one revolution is performed and the hole radius exceeds the cyclotron radius, one obtains

$$N_{rev} < 1; \quad R_c < R_H : S_{dyn} = \frac{1}{2\pi}\left[\psi_{rev}\left(1 - \frac{R_c}{R_H}\right)^2\right.$$
$$\left. + \pi - \psi_{rev} + \phi - \sin\phi - \left(\frac{R_c}{R_H}\right)^2\sin\psi_{rev}\right] \quad (5)$$

Figure 2 shows the transmission coefficient for the cases of no magnetic field and for $B_\parallel$=0.35 T, the field strength at the detector in the quadrupole. The hole radius is 0.395 mm and the diameter:depth aspect ratio is 0.36, resulting in vanishing transmission for $\theta_i > 20$ degrees. For high magnetic field and low electron energy, transmission extends to grazing angles of incidence.
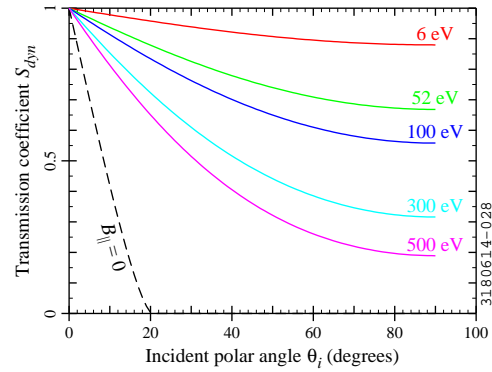

Figure 2: Hole transmission factor S_{dyn} versus incident angle θ_i for the case of no magnetic field (dashed line) and for electron kinetic energies ranging from 6 to 500 eV in a magnetic field of 0.35 T parallel to the hole axis.

The simulated signal charge is calculated as the incident macroparticle charge, Q_{mp}, multiplied by the hole transmission S_H. The charge fraction Q_{wall} which does not enter the holes, $Q_{wall} = (1 - S_\perp)Q_{mp}$, is used to calculate the charge of secondaries produced on the wall in the detector region. The signal charge is summed during a time step to calculate the current, which is then converted to the simulated measured voltage using the amplifier impedance of 50 Ω and gain of 100.

MODELING FOR 20-BUNCH TRAINS

Figure 3 compares the ECLOUD simulation results to the recorded signals for trains of 20 bunches with average bunch populations corresponding to 4.01, 6.26, 7.26, and 8.26 mA/bunch, with 1.6×10^{10} positrons per mA. The 13-MHz filter has been applied to the modeled signal as well as to the oscilloscope trace, with the consequence that the statistical error bars are highly correlated. The abrupt reduction in the signal slope after the passage of the first 6 bunches has been shown to arise from the clearing of cloud electrons which were trapped during the 2.3 μs time interval prior to the return of the bunch train [8]. A subset of the cleared, or ejected, trapped cloud electrons contributes to the stripline
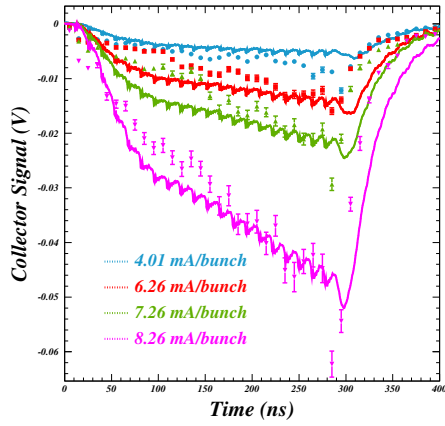
Figure 3: Measured and modeled (points with error bars) shielded stripline detector signals for trains of 20 bunches with average bunch population ranging between 6.4×10^{10} and 13.2×10^{10} positrons.
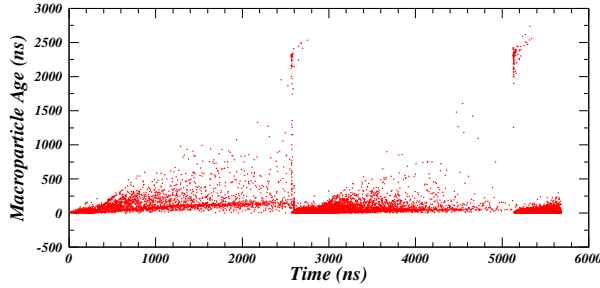

Figure 4: Signal macroparticle age plotted versus modeled cloud development time. The arrival times of the bunch train near 2.5 and 5.1 μs show a class of long-lived macroparticles which are accelerated into the detector by the beam.

signal, as shown in Fig. 4, where the time since the previous wall collision for individual macroparticles is shown as a function of cloud development time. Closer inspection of this macroparticle age, or time-of-flight, distribution shows that the previous wall collision for these trapped electrons occurred near the end of the preceding passage of the train.

The ECLOUD SEY model produces a single macroparticle for each wall collision, choosing the emission process, elastic, re-diffused or true secondary [9] according to its relative probability. In this manner, the original production kinematics remain associated with the macroparticle during the cloud development. Figure 5 shows the positions on the vacuum chamber wall where the signal macroparticles were originally photo-produced. The coordinate s denotes the production position along the circumference of the cylindrical vacuum chamber, with its origin in the horizontal mid-plane on the outside of the ring, proceeding clockwise (see Fig. 1b) along with the azimuthal angle ϕ_s. The center of the detector is located at ϕ_s = 135 degrees. A region extending ±10 mm in front of each of the four magnet poles is shown. The signal is produced primarily by electrons originating near field lines intersecting the detector, i.e. from a narrow region in front of the diametrically opposed pole and from 4-mm-wide regions on the vacuum chamber surface

extending from the centers of the neighboring poles toward the detector, as well as from the ±4 mm region in front of the detector itself. So, while the motion of the cloud electrons accelerated by the beam in the strong field of the quadrupole magnet is complicated, even chaotic in the regions of low field strength, those which contribute to the detector signal are generally confined to regions near the magnetic field lines intersecting the detector region, which are also lines which pass close to the beam.
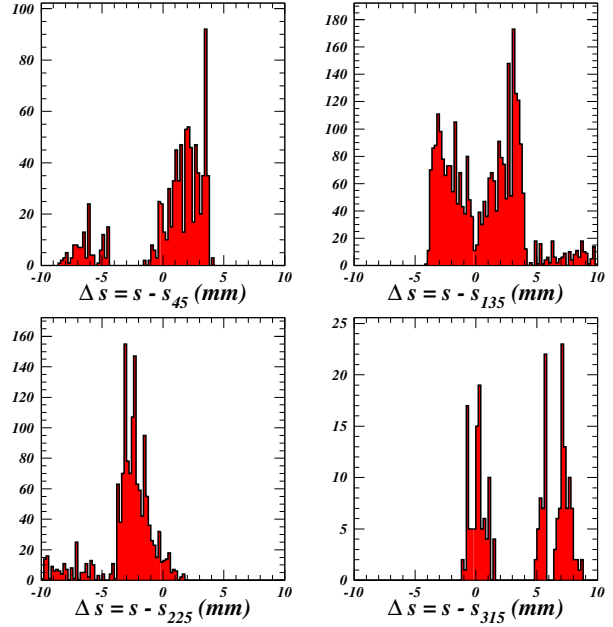

Figure 5: Coordinate Δs where the signal macroparticles were originally photo-produced, relative to the center of each magnet pole.

REFERENCES

[1] G.F. Dugan, M.A. Palmer, and D.L. Rubin, ICFA Beam Dynamics Newsletter No. 50, Eds. J. Urakawa and W. Chou, pp. 11-33 (2009)

[2] F. Zimmermann, G. Rumolo and K. Ohmi, ICFA Beam Dynamics Newsletter No. 33, Eds. K. Ohmi and M. Furman, pp. 14-24 (2004)

[3] J. A. Crittenden *et al.*, Nucl. Instrum. Methods Phys. Res. A **749**, 42 (2014)

[4] J.P. Sikora *et al.*, WEP195, proceedings of PAC2011, March 28 - April 1, 2011, New York City, NY, USA

[5] J.A. Crittenden *et al.*, WEP135, proceedings of IPAC2011, September 4-9, 2011, San Sebastian, Spain

[6] J.A. Crittenden and J.P. Sikora, proceedings of ECLOUD'12, June 5-8, 2012, La Biodola, Isola di Elba, Italy, CERN Report 2013-002, pp. 241-250

[7] J.A. Crittenden *et al.*, MOPWA072, proceedings of IPAC2013, May 13-17, 2013, Shangai, China

[8] M. G. Billing *et al.*, arXiv:1309.2625v3 (2014)

[9] M.A. Furman and M.T.F. Pivi, Phys. Rev. ST Accel. Beams **5**, 124404 (2002)